Tellus (2006), 58B, 218–228
Printed in Singapore. All rights reserved

TELLUS

Aerosol optical depth at ALOMAR Observatory (Andøya, Norway) in summer 2002 and 2003

By CARLOS TOLEDANO[1]*, VICTORIA CACHORRO[1], ALBERTO BERJÓN[1], MAR SORRIBAS[2], RICARDO VERGAZ[1], ÁNGEL DE FRUTOS[1], MANUEL ANTÓN[3] and MICHAEL GAUSA[4], [1]*Grupo de Optica Atmosférica, Universidad de Valladolid, Paseo Prado de la Magdalena s/n, 47071 Valladolid, Spain;* [2]*Instituto Nacional de Técnica Aeroespacial, 21130 Huelva, Spain;* [3]*Universidad de Extremadura, 06071 Badajoz, Spain;* [4]*ALOMAR Observatory, Andøya Rocket Range, N-8483 Andenes, Norway*

(Manuscript received 13 June 2005; in final form 26 January 2006)

ABSTRACT

Two intensive campaigns were carried out by the Atmospheric Optics Group of Valladolid University (GOA-UVA) during summer 2002 and 2003 at ALOMAR station (Andøya island, Norway, 69°16′N, 16°00′E), allowing an aerosol characterization and classification in this coastal Arctic region during the summer. Aerosol measurements were performed with a Cimel sun photometer at the four nominal aerosol wavelengths 440 nm, 670 nm, 870 nm and 1020 nm. Spectral measurements in the range 300–1100 nm with a field spectroradiometer Licor-1800 were also performed during 2003, allowing a comparison with Cimel data. The agreement between both instruments is inside the current error for field aerosol optical depth retrieval, namely, 0.02. Although aerosol optical depth (AOD) at the nominal wavelength of 440 nm has an average value below 0.12, values range from 0.04 to 0.36. Derived Ångström alpha coefficient gives an average value about 1.6 (STD 0.2), meaning predominance of fine particles. These values do not fit the typical maritime aerosol characteristics. Continental and long-range transport air masses seem to influence this area, giving rise to mixed aerosols. Back trajectory analysis shows the predominance of Atlantic air masses with low AOD, while continental air masses show in general larger aerosol loading.

1. Introduction

Aerosols play a major role in radiative transfer processes in the atmosphere and radiative forcing is a key effect in climate change. Therefore, strong efforts are held for global aerosol monitoring and characterization. For this purpose, worldwide photometers networks have been developed (Holben et al., 1998; Werhli, 2000; Bokoye et al., 2001), and many intensive measurement campaigns have been performed: ACE-ASIA (http://www.ogp.noaa.gov/ace-asia), ACE II (Raes et al., 2000), INDOEX (http://www-indoex.ucsd.edu), SAFARI (http://www.wits.ac.za/fac/engineering/-civil/Safari/), and many others. Continuous measurements at specific sites permit aerosol properties characterization and hence the possibility to establish an aerosol climatology (D'Almeida et al., 1991; Holben et al., 2001). The AERONET (Aerosol Robotic Network, http://aeronet.gsfc.nasa.gov) and the PHOTONS (Photometrie pour le Traitement Operationnel de Normalisation Satellitaire, http://www-loa.univ-lille1.fr/photons) projects are excellent examples of the necessary initiatives for studying aerosol characterization in a global scale. They have achieved a great coverage in Europe, America and certain regions of Asia and Africa, covering today practically all parts of the world. However, long-term aerosol data in the Arctic and Antarctic regions are still scarce, and very few sites belonging to established networks are above 60° latitude, which are precisely regions with high risk related with the climate change.

An overview of the history about Arctic aerosol studies can be seen in Barrie (1986) and Shaw (1995). More recent studies, mainly based in optical properties measurements, have been carried out by many authors, by means of ground-based measurements (Radionov et al., 1995; Polissar et al., 1999; Bigg and Leck, 2001; Bokoye et al., 2002; Herber et al., 2002; Quinn et al., 2002; Treffeisen et al., 2004), airborne campaigns (Pacyna and Ottar, 1988; Heintzenberg et al., 1991; Nagel et al., 1998; Yamanouchi et al., 2005) and satellite (Herber et al., 1993; Thomason et al., 2003). Routine aerosol measurements are performed in key sites, for example, Alaska (Bodhaine and Dutton, 1993; Polissar et al., 1999) and Svalbard (Herber et al.,

*Corresponding author.
e-mail: toledano@baraja.opt.cie.uva.es
DOI: 10.1111/j.1600-0889.2006.00184.x

2002; Yamanouchi et al., 2005). On 2003 April, a Cimel sun photometer of the AERONET network was deployed at Longyearbyen, Svalbard, for long-term aerosol monitoring, but it has recently been moved to Hornsund (there are no published data from these sites).

The radiative influence due to Arctic aerosols (Rinke et al., 2004; Treffeisen et al., 2005) is difficult to estimate because of specific reasons such as high surface albedo, long path of solar radiation through the atmosphere and inhomogeneous aerosol distribution. High aerosol concentration during spring (Arctic haze) dominates the seasonal pattern of aerosols in Arctic regions (Shaw, 1982; 1995). Arctic haze is the result of long transport from mid-latitude sources in Russia, Europe and North America (Herber et al., 2002; Heintzenberg et al., 2003).

The aim of this work is to provide an initial characterization of aerosols in the north coast of Norway, as a first step towards the development of an aerosol local climatology in this Arctic region. In this context, two intensive campaigns were carried out by the Atmospheric Optics Group of Valladolid University (GOA-UVA) during summer 2002 and 2003 at ALOMAR station (Andenes, Norway).

Remote sensing instruments for aerosol measurements were deployed at the station, together with the ALOMAR instruments operating routinely. This configuration permitted the determination and comparison of column aerosol optical properties and water vapour content with different methods. In this work aerosol optical depth (AOD) spectral measurements and the derived Ångström coefficient are analysed and linked with air mass back trajectories for a general characterization.

2. Site description, instrumentation and measurements

2.1. Site description

The ALOMAR (Arctic Lidar Observatory for Middle Atmosphere Research) station is located in Andøya island close to Andenes town (69°16′N, 16°00′E, elev. 380 m), on the Atlantic coast of Norway about 300 km north of the Arctic Circle. The facility is managed by the Andøya Rocket Range. From the end of May to the end of July the sun is 24 hr above the horizon, with a maximum elevation during the solstice of 42° at noon and 2° at midnight. The climate is strongly influenced by the Gulf Stream, which provides mild temperatures during the entire year, with average temperature of −2°C in January and 11°C in July. The terrace at the Observatory provides excellent 360° free horizon, suitable for 24 hr continuous direct sun measurements during midnight sun period. During the campaigns warm temperatures up to 20°C were registered, as well as snow showers in late May.

2.2. Instrumentation and measurements

The GOA-UVA instruments deployed at ALOMAR were a Cimel sun photometer during both campaigns and a Licor-1800 field spectroradiometer during the 2003 campaign. The Cimel Electronique CE-318 sun photometer (Cimel-Electronique, 2004) is the standard instrument of AERONET network. It is an automatic sun and sky radiometer, with spectral interference filters (10 nm FWHM) centred in selected wavelengths: 440, 670, 870 and 1020 nm for aerosol measurements. Direct sun measurements are performed at these wavelengths to determine aerosol optical depth and another channel at 940 nm is used for water vapour content retrieval. Three direct sun measurements are performed at each time (triplet) in order to reject cloud contamination. Sky radiance measurements are acquired at the aerosol wavelengths in the solar almucantar and principal plane. Cimel sun photometers were calibrated by intercomparison with an AERONET master instrument. For more details about this instrument see Holben et al. (1998). Inversion algorithms can be then applied to the sky and sun measurements to retrieve aerosol size distribution, single scattering albedo, phase function and refractive index (Dubovik and King, 2000).

Licor-1800 is a commercial field spectroradiometer that covers a spectral range of 300–1100 nm with variable wavelength sampling. Our measurements were sampled at each 1 nm. The monochromator has a holographic grating of 800 grooves/mm and the detector is a silicon photodiode. The nominal spectral resolution checked in our laboratory is 6.2 ± 0.3 nm FWHM (nominal 6 nm). A filter wheel with seven attenuation filters reduces stray light and an opaque target provides dark-signal before and after each irradiance scan. A 2.3° field of view was delimited for direct sun measurements with a collimator system coupled to the Licor cosine receptor. Sun tracking was carried out with an automatic robot completely developed by GOA. Calibration, maintenance and errors associated with the measurements of Licor have been extensively explained elsewhere (Cachorro et al., 2001, 2004; Vergaz et al., 2005).

In summer 2002 Cimel number #243 was deployed, whereas in summer 2003 another sun photometer, number #421, was deployed. The Cimel automatic sequence was followed during the 2002 campaign, thus measurements at air masses below 7 were performed between 2002 May 25 and July 26. This sequence includes direct sun measurements at selected air masses from 7 to 2 and each 15 min when air mass is below 2. Almucantar and principal plane sky radiance measurements are performed each hour. For the 2003 campaign an enhanced measurement schedule was implemented for 24 hr direct sun measurements reaching air masses near 17 (87° solar zenith angle) at midnight; thus the Cimel has proved to have a wide dynamic range. Licor is a manual field spectroradiometer, so measurements were carried out during 14 hr per day in cloud-free conditions.

Cimel #421 and Licor operated together from 2003 June 1 until July 31, and Cimel #421 continued in operation until 2003 September 15. The data were calibrated and processed according to AERONET protocols. Cimel #243 was calibrated in GSFC Facility, NASA (Washington) and Cimel #421 was calibrated in LOA Facilities (Lille-Carpentras, France). All the Cimel data

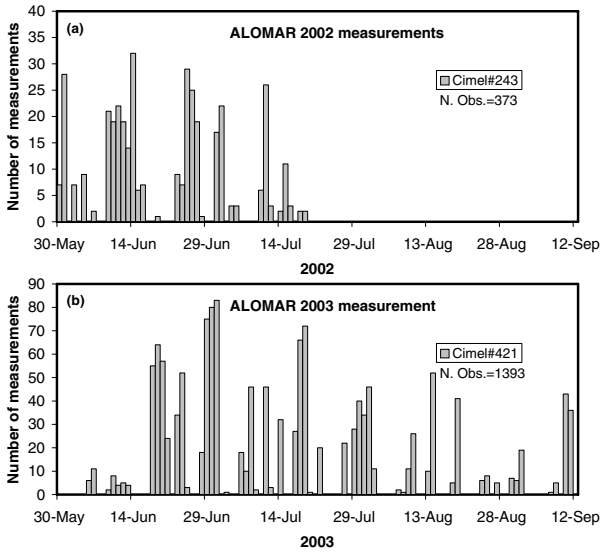

Fig. 1. Number of measurements performed each day in (a) the 2002 campaign and (b) the 2003 campaign with Cimel sun photometer.

are included in the AERONET network in the site 'Andenes', with level 2.0 for the 2002 campaign and level 1.5 for the 2003 campaign. Sky radiance data for the 2003 campaign present some calibration problems that must be solved before using these data.

Weather conditions at ALOMAR permitted 50% of days with measurements (three or more cloud-free observations), during both 2002 and 2003. The number of Cimel measurements performed every day for the 2002 and 2003 campaigns is summarized in Fig. 1, where only cloud-free observations are considered. With the 2002 schedule up to 40 measurements were possible each day and the total number of observations was 373. With the enhanced schedule in 2003, up to 85 measurements were scheduled each day for continuous AOD monitoring, and 1393 observations were performed.

Routine measurements are performed at ALOMAR Observatory with a Brewer MK-II spectroradiometer. The Brewer (number #104) provides total ozone content during the day. The daily average of this ozone content provided by the Brewer was used for spectral AOD retrieval in the 2003 campaign. Ozone content oscillated between 264 and 388 DU. However, differences in Cimel AOD (670 nm channel) between the AERONET processing (with ozone climatological values) and our own processing (using the Brewer measured ozone values), were below 0.008, thus inside the nominal error for field measurements.

3. Theoretical background and methodology

Aerosol parameters are retrieved from direct solar irradiance measurements at ground level. Total optical thickness of the atmosphere (τ) is obtained from the absolute direct solar irradiance (or signal in mA, digital counts, etc.) measured at ground level, $F(\lambda)$, using the Beer-Lambert law:

$$F(\lambda) = F_0(\lambda) \cdot e^{(-\tau \cdot m)},$$

where $F_0(\lambda)$ is the irradiance (or instrument signal) at the top of the atmosphere, corrected by the earth–sun distance, and m is the airmass factor evaluated with the formula by Kasten and Young (1989).

Aerosol optical depth (AOD or τ_a) is obtained from the total optical depth after subtraction of the Rayleigh optical thickness (τ_R) contribution and the ozone optical thickness (τ_{O3}) according to

$$\tau_a = \tau - \tau_R - \tau_{O3}$$

Ozone optical depth contribution and Rayleigh scattering (corrected with pressure at the site level provided by the ALOMAR weather station), were taken into account according to Cachorro et al. (2000).

Spectral AOD data allow the determination of the Ångström coefficient (Ångström, 1930, 1961). This parameter describes the behaviour of the aerosol optical depth with wavelength, which is related to the aerosol size, giving insight about predominance of the fine mode or the coarse mode of aerosols. AOD spectral data are fitted according to the Ångström formula:

$$\tau_a(\lambda) = \beta \cdot (\lambda)^{-\alpha}.$$

With Cimel sun photometer, three channels are used: 440, 670 and 870 nm, thus alpha (440–870) is obtained. With Licor data all wavelengths in the range 300–1100 are available, but only those in non-absorbing windows in the range 370–870 nm are used for alpha determination (Cachorro et al., 2000; Vergaz, 2001).

Direct sun measurements performed by Cimel were cloud screened with the AERONET standard cloud-screening algorithm (Smirnov et al., 2000). Licor measurements were manually performed following the Cimel schedule to facilitate cloud screening. The presence of clouds was also daily registered by the Licor operator for further confirmation.

Absolute error for AOD retrieval with the Cimel sun photometer calibrated within AERONET protocols is 0.01–0.02 (Holben et al., 1998; see also AERONET web page). For Licor the error is also wavelength dependent, larger in UV and IR regions, and in general is below 0.05 (Cachorro et al., 2000; Vergaz et al., 2005). Errors in alpha coefficient strongly depend on AOD errors and AOD absolute values, and in general they can be estimated in the range 10–20%, but larger for low AOD's.

4. Results and discussion

In tropical or mid-latitude sites, maritime aerosol properties are relatively well characterized. In general, pure maritime aerosol will be found in remote island locations, and presents AOD < 0.15 at 500 nm and alpha < 1, (Smirnov et al., 2002, 2003). According to these authors, the AOD (440 nm) would be

below 0.17, considering a typical maritime alpha value of 0.8, although other authors establish alpha below 0.5 (Hess et al., 1998; see ref. in Smirnov et al., 2002). Coastal regions may present influences of different origin (desert, industrial, continental) depending on the site location, so local climatologies are needed for a complete assessment of aerosol properties. A very complete overview about maritime aerosols publications is provided in Smirnov et al. (2002), but few of them refer to North Atlantic and none specifically to the Arctic Ocean. There is a lack of measurements in this Norwegian Arctic region and a specific characterization is needed.

Local aerosol anthropogenic sources are almost absent in the Arctic, and high turbidity is dominated by long transport from source regions, which mainly occurs during late winter and spring (Shaw, 1995). The Arctic haze formation is also related to high stability of the winter Arctic troposphere. Lower AOD values are observed in summer with respect to spring (Herber et al., 2002; Treffeisen et al., 2004). In general, AOD peaks in spring with values around 0.15–0.20 and higher during strong haze episodes. During the summer and autumn, aerosol loading decreases to background values, around 0.05 at 500 nm, similar to Antarctic background AOD (Herber et al., 1996). High colour ratio (ratio between AOD at two wavelengths, similar to the Ångström exponent) is associated with spectral AOD, indicating predominance of fine particles.

About ground-level particles other authors report an increase in the particle number concentration during summer (Ström et al., 2003), which is suggested to be due to a higher biological activity. The study by Tunved et al. (2003) in various Scandinavian sites, also reports higher values of particle number concentration during spring and summer seasons, with a maximum of nucleation events during the spring months. These authors show a predominance of fine particles in the aerosols present in the Arctic regions.

In this study, a detailed analysis of summer AOD and alpha coefficient measured at ALOMAR Observatory (Andenes, Norway) is carried out, giving their general features. Three specific episodes are also analysed to show in detail high, medium and low turbidity events. We have preferred to present the retrieved data for the 2002 and 2003 campaigns separately, for a more detailed analysis of aerosol variability during each campaign.

4.1. Aerosol optical depth and alpha features during the 2002 summer campaign

Statistical results for aerosol optical depth and Ångström alpha parameter during the 2002 summer campaign are summarized in Table 1. The average AOD (440 nm) is 0.13 with standard deviation (STD) of 0.06, which represents 50% of the average value. At 1020 nm channel the average AOD is 0.04 (STD 0.02), thus strong wavelength dependence is observed, as shown by the high average alpha value: 1.6. This variability is consistent for all AOD channels according to the values given in Table 1.

Table 1. General statistics for the 2002 campaign at ALOMAR

N obs = 373 $m < 7$	AOD 1020 nm	AOD 870 nm	AOD 670 nm	AOD 440 nm	Alpha
Average	0.04	0.04	0.06	0.13	1.6
STD	0.02	0.02	0.03	0.06	0.3
Max.	0.19	0.20	0.22	0.36	2.1
Min.	0.01	0.01	0.02	0.04	0.4
Median	0.03	0.04	0.06	0.11	1.7

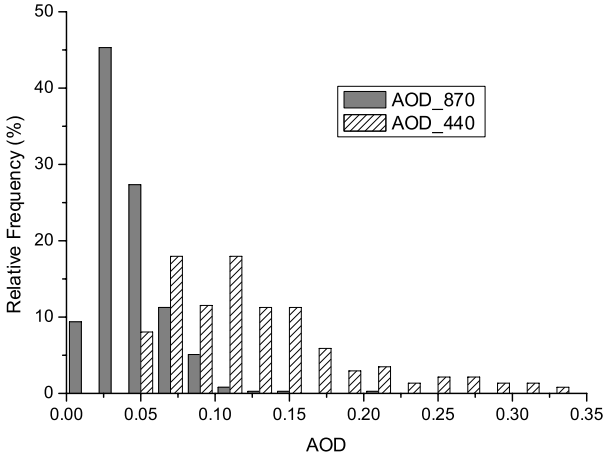

Fig. 2. AOD relative frequencies during the 2002 campaign.

Further statistical information can be extracted from the analysis of the frequency distribution histograms. The frequency distribution for AOD data in 440 and 870 nm channels is shown in Fig. 2. Most of AOD (440 nm) observations (80%) were below 0.17, thus indicating low turbidity, and data are within representative values of maritime aerosol type. The frequency peak for AOD (440 nm) is found at 0.11 and peaks for longer wavelengths are at lower values (see Fig. 2). The 870 nm channel (also 670 nm and 1020 nm, not shown) presents a narrower frequency distribution histogram compared to that of 440 nm.

The results for alpha parameter are also summarized in Table 1. The average value is 1.6, with a relatively small standard deviation (0.3 or 18%). The frequency distribution is presented in Fig. 3, and shows a maximum around 1.7, close to the average value. The most significant result is that 97.5% of the data give alpha values above 1, that is, above the representative threshold for maritime aerosol type according to Smirnov et al. (2003). Furthermore, the lowest alpha values observed may be due to thin cirrus clouds, because of the difficulty of the automatic cloud-screening algorithm to detect them.

Finally, Fig. 4 shows the temporal evolution for AOD (440 nm) and alpha during this 2002 campaign, giving a better

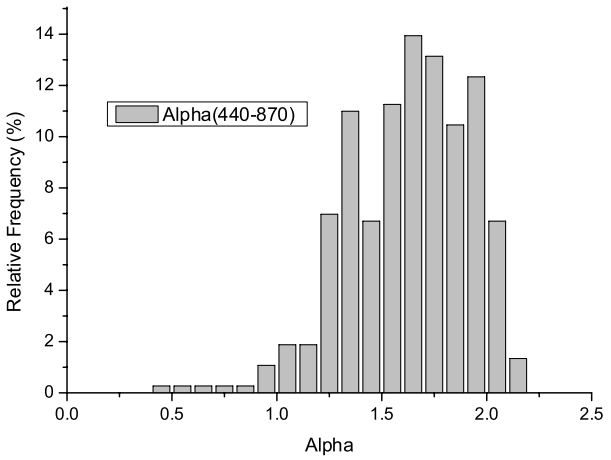

Fig. 3. Alpha relative frequencies during the 2002 campaign.

illustration of aerosol variability. AOD (440 nm) values range from 0.04 to 0.36. Two episodes with AOD as high as 0.3 take place on June 9 and July 11. These high turbidity events also present high alpha values (about 1.7–2), which imply large aerosol loading of fine particles.

4.2. *Aerosol characteristics during summer campaign 2003*

For the 2003 summer campaign we have performed a similar analysis. A general statistics is summarized in Table 2. Note that data in 2003 range from June to middle September, that is, the whole 2003 summer. Average AOD (440 nm) is 0.11 (STD 0.04); lower than the average for the 2002 campaign. The evolution of AOD during summer 2003, presented in Fig. 5, is not as variable as in summer 2002, and most of the days in July and August have AOD (440 nm) below 0.1. Very few observations (less than 2%) were above 0.2 for AOD (440 nm).

The AOD (440 nm) frequency distribution presented in Fig. 6 shows 48% of observations below 0.1 and 90% below 0.17. These results agree with the reported summer low aerosol optical depths in the Arctic (Herber et al., 2002), with an AOD decrease during summer as can be observed in Fig. 5. Mean AOD in 2003

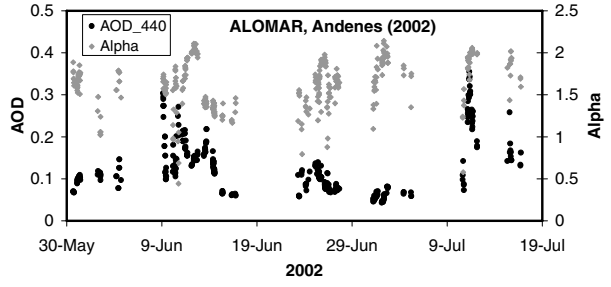

Fig. 4. AOD and alpha during the 2002 campaign.

Table 2. General statistics for the 2003 campaign at ALOMAR

N obs = 1393 $m < 17$	AOD 1020 nm	AOD 870 nm	AOD 670 nm	AOD 440 nm	Alpha
Average	0.03	0.04	0.05	0.11	1.6
STD	0.01	0.01	0.02	0.04	0.2
Max.	0.08	0.09	0.13	0.26	2.0
Min.	0.02	0.02	0.02	0.05	0.6
Median	0.03	0.03	0.05	0.10	1.6

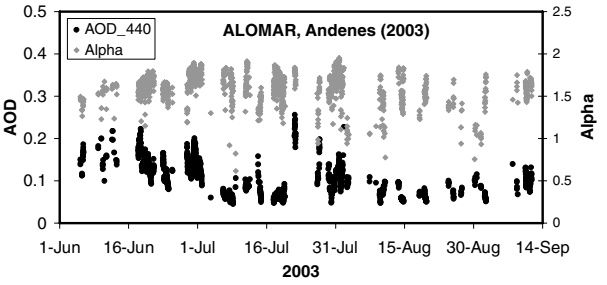

Fig. 5. AOD and alpha during the 2003 campaign.

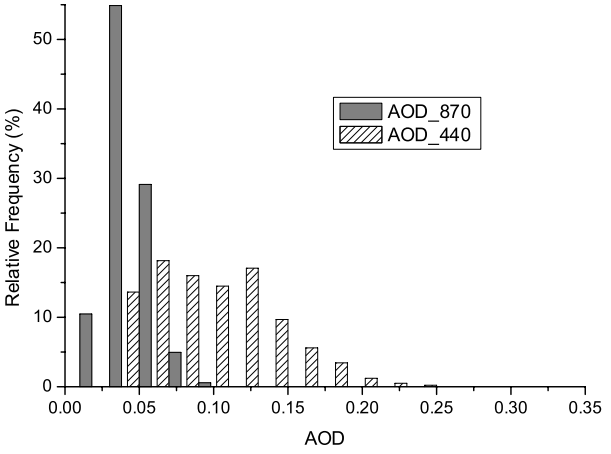

Fig. 6. AOD relative frequencies during the 2003 campaign.

June was 0.14, indicating a moderate pollution level, probably as a result of long transported aerosols across the Arctic, given that back trajectories during June show mostly northerly flows, covering a sector from NE to NW. A lower mean AOD (440 nm) of 0.09 in July and 0.08 in August and September was obtained, although two short episodes (associated with South advections) on July 22 and July 31 registered high AOD.

Ångström exponent in 2003 has an average of 1.6 (STD 0.18), which is very similar to the average alpha during 2002, and with a small variability, typically 11% of the average alpha. The evolution of the Ångström exponent (Fig. 5) shows values mainly between 1.3 and 1.8. The frequency histogram in Fig. 7 shows no significant observations below 1, and a narrow distribution

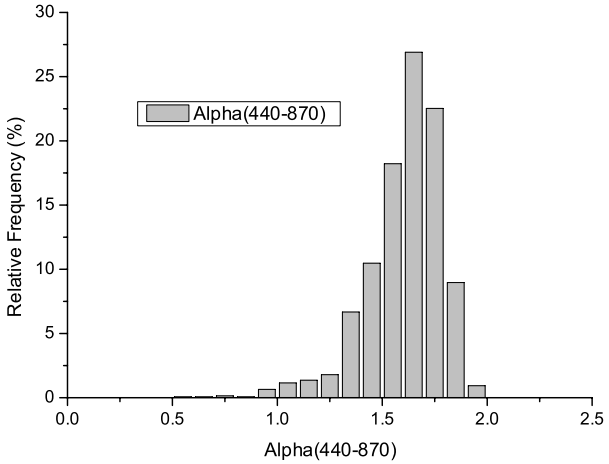

Fig. 7. Alpha relative frequencies during the 2003 campaign.

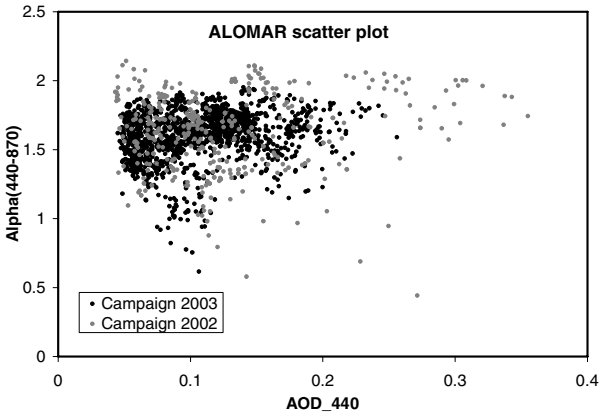

Fig. 9. Scatter plot AOD versus alpha in 2002 and 2003 with Cimel data.

between 1.3 and 1.9 with peak at alpha = 1.7. This is consistent with results from 2002.

As mentioned, during this campaign simultaneous Cimel and Licor measurements are available, and comparative results are obtained in 2003 June and July. The comparison at the 440 nm and 670 nm wavelengths show AOD absolute differences below 0.02 (0.03 for 870 nm), which is the AERONET error threshold specified for field instruments. At 1020 nm the relative differences result near 100% because of low AOD values, but most absolute differences are below 0.05. The average AOD (440 nm) with Licor is 0.129 and that of Cimel for the same operation period (June and July 2003) is 0.125. Averages AOD for the 670 nm wavelength are 0.08 and 0.07 for Licor and Cimel, respectively. Less agreement is obtained for infrared channels as mentioned above. An example of Licor and Cimel data comparison for AOD in 440 nm channel can be seen in Fig. 8. One advantage of Licor data is that we have measurements at UV wavelengths, for example, average AOD at 350 nm was 0.17. These data may be used as reference values for comparison when Brewer AOD data in the UV are available (Groebner et al., 2001; Groebner and Meleti, 2003).

The scatter plot of AOD versus alpha is a common tool for aerosol measurements analysis and Fig. 9 reflects clearly that

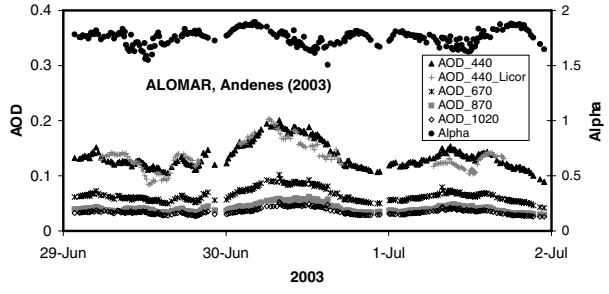

Fig. 8. AOD and alpha for 2003 June 29 to July 1, at ALOMAR.

for all AOD range, alpha values greater than 1 are observed. A first look of this plot seems to indicate continental aerosol type, except for the low measured AOD. The region with AOD greater than 0.17 and high alphas usually means continental or polluted-continental aerosol type (Holben et al., 2001). The region with AOD below 0.17 and alphas greater than 1 is discussed below.

Although AOD retrievals during both campaigns are in good agreement with AOD reported by Herber et al. (2002), alpha parameter presented by these authors at Svalbard is much smaller (mean value 0.8 in summer and 1.0 in spring). One possible explanation is the large uncertainties in alphas associated with low optical depths and the different spectral range considered. The alphas reported by the AERONET Cimel operating at Longyearbyen (Svalbard), that are directly comparable with our data, present mean value of 1.5 (STD 0.4), which is in good agreement with our results at Andøya. At Longyearbyen, the AOD (440 nm) mean value was 0.18 in June, 0.09 in July and 0.06 in August and September 2003; thus strong correlation was found between both Arctic sites, also in agreement with the expected low AOD values in summer and autumn. The mentioned high turbidity episode in 2003 June was also recorded at Longyearbyen, since the turbid air mass arriving at Andøya from NE was also over passing Svalbard.

The above results of AOD and alpha parameters from the 2002 and 2003 campaigns clearly show that the analysed aerosols are not within the cited reference values for maritime aerosol type. Although AOD values are inside the maritime coastal aerosol range (low turbidity in general), the alpha values are far from it (98.7% of data above alpha = 1). These alpha results indicate fine particles predominance in the aerosol size distribution, according to the criterion for columnar volume size distributions given by Dubovik et al. (2002). These fine particles in moderate–high turbidity events are expectable, both for continental or long-range transported anthropogenic aerosols. However, the presence of fine particles is difficult to explain for low turbidity (mainly maritime) conditions. Recent publications

Table 3. AOD, alpha and water vapour statistics for the sectors in the back trajectory analysis

Sector	Frequency Occurr.	AOD 870 nm	AOD 440 nm	Alpha	Water (cm)	Frequency AOD (440) < 0.1
SW–NW	45–50%	0.032	0.091	1.54	1.00	71%
N–NE	15–20%	0.039	0.114	1.58	0.89	30%
E–S	30–35%	0.038	0.119	1.67	1.45	32%

suggest that these fine particles might be due to bubble bursting of small insoluble organic particles from the surface microlayer of the ocean (Leck and Bigg, 2005a,b). The predominance of Atlantic air masses (as described later)—and sea salt deposition on instruments—indicates a maritime character of background aerosol in this coastal site, supporting the earlier hypothesis about the maritime origin of the fine particles. However, we cannot discard an important influence of continental aerosols over this coastal area, giving rise to mixed aerosol type.

4.3. Back trajectory analysis

Back trajectory analysis has been performed for Cimel data for both data sets (2002 and 2003 campaigns). Trajectories were online calculated with HYSPLIT model (Draxler and Rolph, 2003; Rolph, 2003), considering 5 d (120 hr) back from 12 GMT at each day, at three different levels (500, 1500 and 3000 m amsl) and using the model vertical velocity. HYSPLIT 5 d back trajectories were classified according to air mass origin in three types: SW–NW, N–NE and E–S. These sectors are related to typical synoptic situations in the site. Air masses from southwest to northwest arrive before and after low-pressure systems from the Atlantic, and in principle they can be labelled as maritime. Air masses from north to northeast are also maritime but with strong Arctic character because they are very cold and dry. The last type (east to south) includes warm air masses arriving at the site when high-pressure systems are situated over north Scandinavia or Russia. Note that only days with solar measurements are considered in this study, which means days with few clouds or cloudless days.

This air masses classification is related with the aerosol type and loading. Air masses from E–S (30–35% frequency) have in general larger aerosol loading, with 68% of observations above 0.1 in 440 nm (Table 3). High AOD episodes may occur with transport from central Europe, as the case analysed in Section 4.4.1. The Ångström coefficient is also above the average 1.6, thus fine particles transport or continental aerosols may be associated with these air masses. Cimel provides water vapour content in the atmospheric column (Bruegge et al., 1992; Holben et al., 1998), and these data have been used for air mass discrimination. Mean water vapour content was 1.45 cm (STD 0.52 cm). Water vapour content in this group (east to south) is 20–30% higher than the average value, and the highest water contents during both campaigns were associated with these air masses.

Air masses from SW–NW (45–50% occurrence) are usually cloudy and rainy. Most of days without measurements are associated with Atlantic air masses. Aerosol AOD-alpha parameters and water vapour features in these air masses (see Table 3) are very close to the average values, as this is the dominant situation. They have in average low AOD with 71% of measurements below 0.1 (440 nm), and the cleanest days, when background AOD is registered, are associated with them.

Air masses from N–NE (15–20% frequency) are cold and not as clean as expected, since long transport episodes of polluted aerosols from north Russia seem to be associated with these air masses. Aerosol loading is in average similar to the Atlantic maritime air masses, but water vapour is significantly lower, about 35% with an average below 1 cm. North–northeast air masses (Table 3) also present alpha slightly below the average. AOD (440 nm) is always below 0.2 in this group. However, almost 70% observations are above 0.1, which suggests the contribution of long transport across the Arctic Ocean.

According to the back trajectories analysis, air masses of maritime character are predominant, with AOD (440 nm) below 0.1 and alpha in the range 1.3–1.8, which are not representative of maritime aerosols. To explain these unexpected values, further studies seem to be necessary, although the results given by Leck and Bigg (2005a; 2005b) are a new insight. Mixed maritime air masses may reach AOD (440 nm) up to 0.2 but with associated Ångström exponent below 1.7. Continental and polluted aerosols present AOD above 0.1 and alpha above 1.6, and they are mainly associated with air masses arriving at Andenes from Russia and central Europe, that is, transported from mid-latitude regions.

4.4. Detailed analysis of selected episodes

4.4.1. High turbidity episode in July 2002. The highest turbidity measured at Andenes in both campaigns was registered on 2002 July 11. Cimel observations in the four channels and Ångström exponent are shown in Fig. 10. The average value for AOD (440 nm) was 0.28 (STD 0.04). Average value for of alpha was 1.93, which means that mainly fine particles were responsible for the strong attenuation. Other days also present such high alpha values, but in those days AOD was medium–low. It was an exceptional situation, produced by an air mass arriving at the site from south Europe and may be considered as an Arctic haze episode in summer.

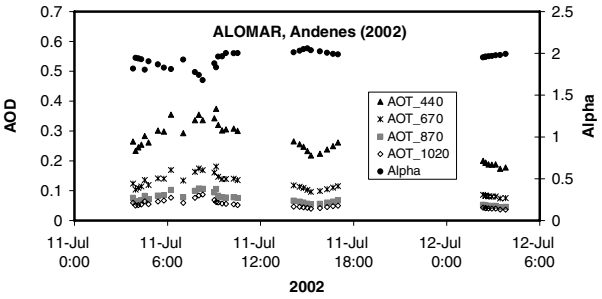

Fig. 10. AOD and alpha for 2002 July 11 and 12, at ALOMAR.

The sky was visually very bright and some cirrus clouds were also present during this meteorological situation. Visibility was highly reduced since the Senja island located 40 km far from the station was not visible. Moreover the backscatter signal from all the ALOMAR Lidar systems was reduced to one-third of current values. Although the earlier observations are mostly qualitative, the conditions during the episode were clearly singular.

During this episode, in order to eliminate cirrus cloud contamination in AOD data, a detailed analysis of ALOMAR Ozone Lidar profiles was performed. Homogeneous and thin cirrus clouds were detected from 8:00 to 10:00 GMT on 11 July. The cloud presence is also detected by the AOD and alpha parameter. A decrease from 2 to 1.6 in alpha is detected from 7:00 to 9:00, with an increase of about 0.03–0.04 in AOD at all wavelengths. Note that direct sun Cimel observations point at as elevation of 35° and Lider observations point at the zenith, so a time delay in clouds presence is expectable from both data.

Low pressure over the Atlantic and high pressure over Scandinavia produced southerly winds in the study area and warm sunny weather (18°C). The HYSPLIT back trajectory analysis shows an air mass going through all Europe from south to north, in all the three levels (550, 1500 and 3000 m amsl), as shown in Fig. 11.

Water vapour retrieval on July 11 presented the highest values during the 2002 campaign, with an average of 2.8 cm. A warm front arrived on July 12, which explains the cirrus presence and increasing relative humidity, and the AOD decreased to 0.18 (440 nm), that is, less aerosol loading, but alpha remains around the same values, so it was the same type of aerosol. Afterwards, the measurements stopped because of rain showers and fog.

A criterion was defined to evaluate turbid episodes for the two campaigns. According to Herber et al. (2002), the mean AOD value + 2 STD was defined as a threshold. The frequency of high turbidity events during summer 2002 and 2003 was 3.6%, mostly registered in June and July, close to the reported 4% by Herber et al. (2002) for the period 1991–1999, but less frequent than the 10% of turbid events reported by Heintzenberg et al. (1991).

4.4.2. 3 d of continuous measurements in 2003 July. It is not frequent to find three consecutive clear sky days at Andøya. The sun was 24 hr per day above the horizon and continuous direct sun measurements were possible for almost 72 hr. These weather conditions were produced by a high-pressure system over north Scandinavia. The air mass remained over the same area for some days, and the back trajectory shows a clockwise pattern arriving at ALOMAR station from the East (Fig. 12).

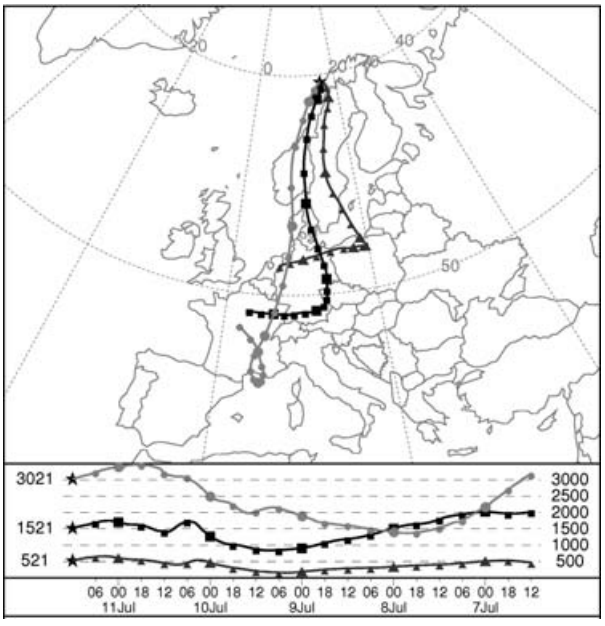

Fig. 11. 5 d back trajectory ending at ALOMAR on 2002 July 11, at 12 GMT.

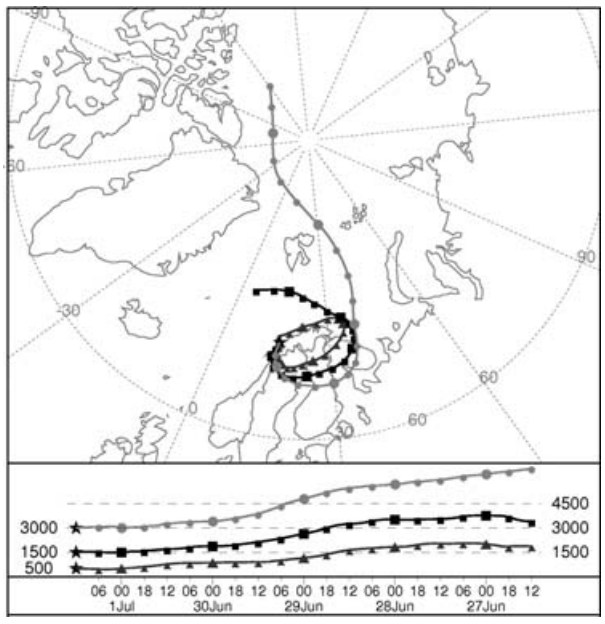

Fig. 12. 5 d back trajectory ending at ALOMAR on 2003 July 1, at 12 GMT.

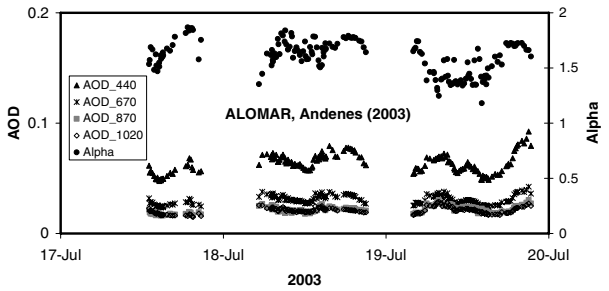

Fig. 13. AOD and alpha for 2003 July 17 to 19, at ALOMAR.

Cimel and Licor (the latter only in 440 nm) measurements in this episode are shown in Fig. 8. The aerosol optical depth presents medium values, with an average AOD (440 nm) of 0.12, 0.16 and 0.13 on June 29, 30 and July 1, respectively. The AOD was over the average 0.11 (440 nm) of the campaign data. Alpha average for the 3 d was 1.75, also above the average alpha for the campaign (1.6). Although alpha is not very stable, no significant changes during the episode were registered. In this episode a continental air mass and dry weather over the site provided these AOD and alpha retrievals higher than the mean values in summer 2003.

4.4.3. Low turbidity episode: summer background conditions. These 3 d constitute a very clean atmosphere episode in the site. Aerosol loading is very close to the lowest values observed during the campaigns (0.05 in 440 nm), thus very close to background aerosol. Data for this episode are presented in Fig. 13. Because of the fog during the 'night' hours, no continuous measurements were possible in this episode.

The AOD (440 nm) daily averages are 0.06, 0.07 and 0.06, respectively. In 1020 nm channel daily averages are about 0.02 for the 3 d. These are typical summer background values, in agreement with the 0.058 at 532 nm reported in the cited work by Herber et al. (2002).

These AOD retrievals are similar to the absolute error in AOD (∼0.01–0.02) estimated for the Cimel sun photometer. It means that relative uncertainty is close to 100%, which affects alpha retrievals. As it can be observed in Fig. 13, alpha is not very stable, because errors in alpha depend on the inverse of AOD (Toledano, 2005). However, daily averages for alpha are 1.7, 1.7 and 1.5, very close to the average alpha for the whole campaign. Water vapour content (0.80 cm) was low compared to the whole data series.

In this episode, sunny weather was assured by a high-pressure system centred south of the site. Back trajectory analysis in Fig. 14 shows an air mass arriving from the west, which is representative of the Atlantic air masses that are predominant in the site.

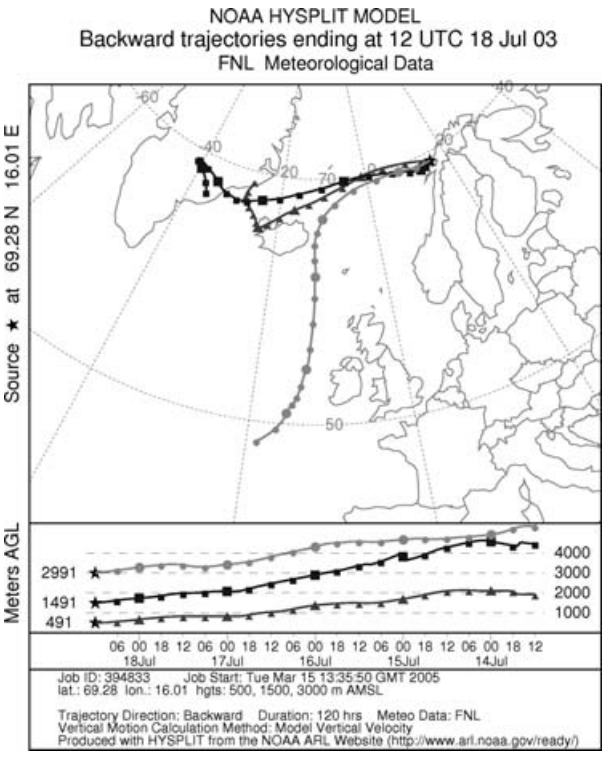

Fig. 14. 5 d back trajectory ending at ALOMAR on 2003 July 18, at 12 GMT.

5. Conclusions

Aerosol measurements were performed at ALOMAR observatory during summer 2002 and 2003, allowing a first characterization by means of AOD and alpha parameters. Maritime aerosol characteristics were expected, mainly when Atlantic air masses are prevailing in this coastal site. Nevertheless under all turbidity conditions, both for low and high AOD values, the alpha parameter shows high values, above 1, indicating predominance of fine particles, not representative in principle of maritime aerosol type. These values for low turbidity conditions are not easy to explain, and further studies are necessary to confirm the origin of these fine particles. Some recent works propose these particles to have a biogenic origin. Moreover, the influence of these particles over columnar aerosol properties must be further investigated.

Back trajectory analysis revealed a close relation between Atlantic air masses and the predominant aerosol properties. Air masses arriving at the site from the south to the east are related to higher aerosol loading, with advection of continental fine particles. Air masses from N to NE are related to long transport of aerosols from source regions in north Russia.

6. Acknowledgments

The ALOMAR ARI and eARI (Enhanced Access to Research Infrastructure) Projects, under the EU's 5th framework programme (FP), and CICYT (Acciones Especiales REN2001-5024-E; REN2002-12641-E/CLI) and REN 2002-00966/CLI provided the necessary funding and infrastructure for the

campaigns. We thank ALOMAR team for their help and dedication. Thanks are also due to AERONET and PHOTONS team for instrument calibration and technical support, especially to B. Holben, I. Slutsker, P. Goloub, B. Damiri and L. Blarel. We acknowledge the NOAA Air Resources Laboratory (ARL) for the provision of the HYSPLIT transport model and READY website, (http://www.arl.noaa.gov/ready.html) used in this publication.

References

Ångström, A. 1930. On the atmospheric transmission of sun radiation II. *Geogr Annales* **H 11**, 1301–1308.

Ångström, A. 1961. Techniques of determining the turbidity of the atmosphere. *Tellus* **13**, 214–223.

Barrie, L.A. 1986. Arctic air pollution monitoring: an overview of current knowledge. *Atmos. Environ.* **15** (20), 643–663.

Bigg, E.K. and Leck, C. 2001. Properties of the aerosol over the central Arctic ocean. *J. Geophys. Res.* **106**(D23), 32 101–32 109.

Bodhaine, B. A. and Dutton, E. G. 1993. A long term decrease in arctic haze at Barrow, Alaska. *Geophys. Res. Lett.* **20**, 947–950.

Bokoye, A. I., Royer, A., O'Neill, N. T., Fedosejevs, G., Teillet, P. M., and co-authors. 2001. Characterization of atmospheric aerosols across Canada. Assessment from a ground-based Sun-photometer network: AEROCAN. *Atmosphere-Ocean* **39**(4), 429–456.

Bokoye, A. I., Royer, A., O'Neil, N. T. and McArthur, L. J. B. 2002. A North American Artic Aerosol Climatology using ground-based sunphotometry. *Arctic (Journal of the Institute of North America)* **55**, 215–228.

Bruegge, C. T., Conel, J. E., Green, R. O., Margolis, J. S., Holm, R. G. and co-authors. 1992. Water vapor column abundance retrievals during FIFE. *J. Geophys. Res.* **97**, 18 759–18 768.

Cachorro, V., Durán, P., Vergaz, R. and de Frutos, A.M. 2000. Measurements of the atmospheric turbidity of the north-center continental area in Spain: spectral aerosol optical thickness and Ångström turbidity parameters. *J. Aerosol Science* **31**, 687–702.

Cachorro, V., Vergaz, R. and de Frutos, A. M. 2001. A quantitative comparison of alpha- turbidity parameter retrieved in different spectral ranges based on spectroradiometer solar radiation measurements. *Atmos. Environ.* **35**, 5117–5124.

Cachorro, V., Vergaz, R. and de Frutos, A. M. 2004. Determination, monitoring and comparison of atmospheric components: aerosol parameters (aerosol optical depth and radiative properties) and water vapor content. In: *First Iberian UV-VIS Instruments Intercomparison: Final Report* (edsSanchez Muniosguren, L., Cuevas, E., de la Morena, B.A.). Technical report, Instituto Nacional de Meteorología, Ministerio de Medio Ambiente, Madrid, Spain.

Cimel-Electronique. *Sunphotometer User manual version 4.6*. April 2004. Cimel Electronique, Paris.

D'Almeida, G., Koepke, P. and Shettle, E. P. 1991. *Atmospheric Aerosol: Global Climatology and Radiative Characteristics*. A Deepak Publishing Hampton, VA, USA.

Draxler, R. and Rolph, G. 2003. Hysplit (HYbrid Single-Particle Lagrangian Integrated Trajectory) model access via NOAA ARL Ready website (http://www.arl.noaa.gov/ready/hysplit4.html). Technical report, NOAA, 2003.

Dubovik, O. and King, M. 2000. A flexible inversion algorithm for retrieval of aerosol optical properties from sun and sky radiance measurements. *J. Geophys. Res.* **105**(D16), 20 673–20 696.

Dubovik, O., Holben, B. N., Eck, T. F., Smirnov, A., Kaufman, Y. J. and co-authors. 2002. Variability of absorption and optical properties of key aerosol types observed in worldwide locations. *J. Atm. Sci.* **59**, 590–608.

Groebner, J., Vergaz, R., Cachorro, V. E., Redondas, A., Henriquez, A. and co-authors. 2001. Intercomparison of aerosol optical depth measurements in the UVB using Brewer spectrophometers and a Licor spectrophotometer. *Geophys. Res. Lett.* **28** (9), 1691–1694.

Groebner, J. and Meleti, C. 2003. Aerosol optical depth in the UVB and visible from Brewer spectrophotometer direct irradiance measurements: 1991 to 2002. *J. Geophys. Res.* **108**, D24, 4800, doi:10.1029/2003JD.

Heintzenberg, J., Strom, J. and Ogren, J. A.. 1991. Vertical profiles of aerosol properties in the summer troposphere of central Europe, Scandinavia and the Svalbard region. *Atm. Environ.* **25A**, 621–627.

Heintzenberg, J., Tuch, T., Wehner, B., Wiedensohler, A., Wex, H. and co-authors. 2003. Arctic haze over central Europe. *Tellus* **55B**, 796–807.

Herber, A., Thomason, L. W., Radionov, V. F. and Leiterer, U. 1993. Comparison of trends in the tropospheric and stratospheric aerosol optical depths in the Arctic. *J. Geophys. Res.* **98**, 18 441–18 447.

Herber, A., Thomason, L. W., Dethloff, K., Viterbo, P., Radionov, V. F. and co-authors. 1996. Volcanic perturbation of the atmosphere in both polar regions: 1991–1994. *J. Geophys. Res.* **101**, 3921–3928.

Herber, A., Thomason, L. W., Gernandt, H., Leiterer, U., Nagel, D. and co-authors. 2002. Continuous day and night aerosol optical depth observations in the Arctic between 1991 and 1999. *J. Geophys. Res.* **107**(D10), 4097, doi:10.1029/2001JD000536.

Hess, M., Koepke, P. and Schult, I. 1998. Optical properties of aerosols and clouds: The software package OPAC. *Bulletin of the American Meteorological Society* **79**(5), 831–844.

Holben, B., Eck, T., Slutsker, I., Tanré, D., Buis, J. and co-authors. 1998. AERONET- a federated instrument network and data archive for aerosol characterization. *Remote Sens. Environ.* **66**, 1–16.

Holben, B., Tanre, D., Smirnov, A., Eck, T., Slutsker, I. and co-authors. 2001. An emerging ground-based aerosol climatology: Aerosol optical depth from AERONET. *J.Geophys. Res.* **106**, 12 067–12 097.

Kasten, F. and Young, A. T.. 1989. Revised optical air mass tables and approximation formula. *Appl. Opt.* **28**, 4735–4738.

Leck, C. and Bigg, E. K. 2005a. Biogenic particles in the surface microlayer and overlaying atmosphere in the central Arctic Ocean during summer. *Tellus* **57B**(4), 305–316.

Leck, C. and Bigg, E. K.. 2005b. Source and evolution of the marine aerosol—A new perspective. *Geophys. Res. Lett.* **32**, L19803, doi:10.1029/2005GL023651.

Nagel, D., Herber, A., Thomason, L.W. and Leiterer, U. 1998. Vertical distribution of the spectral aerosol optical depth in the Arctic from 1993 to 1996. *J. Geophys. Res.* **103**(D2), 1857–1870.

Pacyna, J. and Ottar, B. 1988. Vertical distribution of aerosols in the Norwegian Arctic. *Atm. Environ.* **22**(10), 2213–2222.

Polissar, A. V., Hopke, P. K., Paatero, P., Kaufmann, Y. J., Hall, D.K. and co-authors. 1999. The aerosol at Barrow, Alaska: long-term trends and source locations. *Atmospheric Environment* **33**, 2441–2458.

Quinn, P. K., Miller, T. L., Bates, T. S., Ogren, J.A., Andrews, E. and co-authors. 2002. A 3-year record of simultaneously measured aerosol chemical and optical properties at Barrow, Alaska. *J. Geophys. Res.* **107**(D11), 4130.

Radionov, V. F., Marshunova, M. S., Rusina, Y. N., Lubo-Lesnichenko, K. Y. and Pimanova, Y.Y. 1995. Atmospheric aerosol turbidity over polar regions. *Atmospheric and Oceanic Physics* **30**(6), 762–766.

Raes, F., Bates, T., McGovern, F. and Liederkeke, M. 2000. The second aerosol characterization experiment (ACE2): general context and main results. *Tellus **52B***, 111–126.

Rinke, A., Dethloff, K. and Fortmann, M. 2004. Regional climate effects of Arctic Haze. *Geophys. Res. Lett.* **31**, L16202, doi:10.1029/2004GL020318.

Rolph, G. 2003. Real-time environmental applications and display system (Ready) website (http://www.arl.noaa.gov/ready/hysplit4.html). Technical report, NOAA.

Shaw, G.E. 1982. Atmospheric turbidity in the polar regions. *J. Appl. Meteor.* **21**, 1080–1088.

Shaw, G.E. 1995. The arctic haze phenomenon. *Bull. Am. Meteorol. Soc.* **76**, 2403–2413.

Smimov, A., Holben, B. N., Eck, T. F. and Dubovik, O. 2000. Cloud-screening and quality control algorithms for the AERONET database. *Remote Sens. Environ.* **73**, 337–349.

Smirnov, A., Holben, B., Kaufman, Y., Dubovik, O., Eck, T. and co-authors. 2002. Optical properties of atmospheric aerosol in maritime environments. *J. Atm. Sci.* **59**, 501–523.

Smirnov, A., Holben, B. N., Dubovik, O., Frouin, R., Eck, T. F. and co-authors. 2003. Maritime component in aerosol optical models derived from Aerosol Robotic Network data. *J. Geophys. Res.* **108**(D1), 4033, doi:10.1029/2002JD002701.

Ström, J. J., Umegård, K., Tørseth, P., Tunved, H.-C., Hansson, K. and co-authors. 2003. One year of particle size distribution and aerosol chemical composition measurements at the Zeppelin Station, Svalbard, March 2000–March 2001. *Physics and Chemistry of the Earth* **28**, 1181–1190.

Thomason, L.W., Herber, A. B., Yamanouchi, T. and Sato, K. 2003. Arctic study on tropospheric aerosol and radiation: comparison of tropospheric aerosol extinction profiles measured by airborne photometer and SAGE II. *Gephys. Res. Lett.* **30**, 1328–1331.

Toledano, C. 2005. Aerosol climatology by means of optical properties and air masses characterization at 'El Arenosillo' AERONET site. Doctoral Thesis. Valladolid University, Valladolíd, Spain.

Treffeisen, R., Herber, A., Strom, J., Shiobara, M., Yamagata, T.Y. and co-authors. 2004. Interpretation of Arctic aerosol properties using cluster analysis applied to observations in the Svalbard area. *Tellus* **56B**(5), 457–476.

Treffeisen, R., Rinke, A., Fortmann, M., Dethloff, K., Herber, A. and co-authors. 2005. A case study of the radiative effects of Arctic aerosols in March 2000. *Atm. Environ.* **39** (5), 899–911.

Tunved, P., Hansson, H.-C., Kulmala, M., Aalto, P., Viisanen, Y., Karlsson, H. and co-authors. 2003. One year boundary layer aerosol size distribution data from five nordic background stations. *Atmos. Chem. Phys.* **3**, 2183–2205.

Vergaz, R. 2001. Propiedades ópticas de los aerosoles atmosféricos. Caracterización del área del Golfo de Cádiz. PhD thesis, Universidad de Valladolid, Valladolíd, Spain.

Vergaz, R., Cachorro, V.E., de Frutos, A.M., Vilaplana, J.M. and de la Morena, B.A. 2005. Columnar characteristics of aerosols in the maritime area of the Cadiz Gulf (Spain). *Int. J. Climatol.* **25**, 1781–1804.

Werhli, C. 2000. Calibration of filter radiometers for determination of atmospheric optical depth. *Metrologia* **37**, 419–422.

Yamanouchi, T., Treffeisen, R., Herber, A., Shiobara, M., Yamagata, S. and co-authors. 2005. Arctic Study of Tropospheric Aerosol and Radiation (ASTAR) 2000: Arctic haze case study. *Tellus* **57B**, 141–152.